Chemical order in the glassy As_xS_{1-x} system: An x-ray-absorption spectroscopy study

C. Y. Yang,* M. A. Paesler, and D. E. Sayers
Department of Physics, North Carolina State University, Raleigh, North Carolina 27695-8202
(Received 21 October 1988)

We have examined chemical ordering in the glassy As_xS_{1-x} system by determining the effect of composition on the local structure of these chalcogenide glasses using x-ray-absorption spectroscopy. Structural changes associated with composition indicate that with increasing S content, the S-rich glasses on the As site have a similar local structure to crystalline As_2S_3 (orpiment), but the As—S—As linkages are replaced by As—S—S linkages at higher S concentration. In As-rich glasses a breakdown of the local AsS_3 configuration is evident and the formation of As—As bonds is observed. Further comparison between As-rich alloys and crystalline As_4S_4 (realgar) suggests that a significant fraction of disordered As_4S_4 molecular fragments is contained in the As-rich region.

I. INTRODUCTION

In discussions of the solid state, an important issue one must often confront is whether the material under consideration is ordered or disordered. Beyond the frequently subtle distinction between crystallinity and amorphicity lie questions about various kinds of order. One particular type of order that comes into play when one is considering a solid comprised of more than one element is *chemical* order. This notion of chemical order deals with the chemical bonds in a disordered system and the bond statistics they follow. A system with a purely statistical distribution of bonds—and thus *no* chemical order—can have a decidedly different character than a system where the chemistry of the constituent elements influences the bond statistics and thereby the properties of the material. Such a system, in which local-chemical-bonding considerations shift the bonding of the solid away from a purely statistical distribution, is said to exhibit chemical order. In the present paper, we deal with a material where chemical order lies at the heart of one's understanding of the properties of the system. Our studies focus on a well-studied chalcogenide glass: arsenic sulfide.

We begin by briefly discussing the notion of chemical order before applying our discussion to arsenic chalcogenide glasses in general and finally to arsenic sulfide in particular. Arsenic chalcogens are of the form As_xC_{1-x} where C is a group-VI*B* element (oxygen, sulfur, selenium, tellurium, or polonium) and $0<x<1$. The principal results—presented in the Results and Discussion section—deal with x-ray-absorption spectroscopy (XAS) data. We discuss these data for samples that are stoichiometric arsenic sulfide (As_2S_3) as well as those that are arsenic rich ($x>0.4$) and sulfur rich ($x<0.4$). Our results lead us to conclusions about the degree of molecular integrity in samples of various composition, and how this molecular nature can affect the properties of the samples under consideration.

In most stable covalent-bonding configurations for bulk-quenched glasses, an atom with N valence electrons is coordinated by the $8-N$ rule such that it would have a completely filled outer shell of electrons. Two disparate models which fulfill the $8-N$ rule represent extremes in the distribution of bond types in a multielemental covalent network. In the *covalent random network* (CRN), bonds occur between homopolar (like or "wrong") and heteropolar (unlike) atomic pairs in a statistically random manner.[1,2] The distribution of types of atomic pairs is not influenced by the relative bond strength. At the other extreme, the *chemically ordered network* (CON) favors lower-energy bonds. The distinction between these two bonding extremes in disordered covalent solids has been clearly drawn by others.[3]

The structures of binary alloys of the As_xS_{1-x} system are of considerable interest for several reasons besides the question of whether they are best represented by a CRN or a CON model. Although the As-S system has a large glass-forming region, it is well known that very small compositional changes can give rise to drastic structural changes near stoichiometry ($x=0.4$). For example, glass-transition temperatures[4,5] as well as optical gaps[6,7] are strongly composition dependent. A sharp maximum in a plot of the glass transition temperature T_g versus composition occurs at the stoichiometric compound As_2S_3. T_g decreases monotonically for both S-rich ($x<0.4$) and As-rich ($x>0.4$) samples. Optical studies reveal an optical gap that increases monotonically with S content as x falls from 0.4 to 0. For As-rich glasses in the glass-forming region, the gap decreases with increasing As content. From these results and others, a number of investigators[3–7] have concluded that knowledge of the statistics of chemical bonding is an important key to understanding the compositional dependence of the physical and optical properties of As_xS_{1-x} alloys.

To address chemical ordering in the As_xS_{1-x} system one must first consider the species that are known to occur in the As-S system. A number of such stable species are known to occur in crystalline (c-) As_xS_{1-x} compounds. These include the AsS_3 units in crystalline As_2S_3 or orpiment, the As_4S_4 molecules in c-As_4S_4 or realgar, the As_4S_3 molecules in c-As_4S_3 or dimorphite, and S_8 molecules in c-S. From a chemical bonding viewpoint, the As atom with $4p$ electrons fills the octet

rule with coordination of three. The orbitals of twofold-coordinated S form only two p bonds in their lowest-energy configurations. Thus AsS_3, As_4S_4, and As_4S_3 species may be expected to have highly stable bonding configurations with threefold-coordinated As and twofold-coordinated S. In strongly S-rich alloys, S_8 molecules might likewise be expected.

In the CRN model, the As_xS_{1-x} system includes a statistical mix of As—As, As—S, and S—S bonds at all compositions except $x=1$ and $x=0$. The CON model assumes that only As—S and S—S bonds are contained in S-rich alloys ($x<0.4$), while only As—S and As—As bonds are allowed for As-rich alloys ($x>0.4$). At all compositions, the CON model allows for the existence of any of the above-mentioned structural units, with the relative number of each of the units commensurate with the overall composition of the alloy itself.

Chemical ordering in arsenic sulfide relates ultimately to the correlation between structure and chemical composition in As_xS_{1-x} alloys. The investigation of this correlation through XAS techniques constitutes the central issue in the present study. In considering the compositional dependence of local structure, three important questions provide the main focus of our investigation. (1) What structural model is consistent with the present XAS results in describing the distribution of all types of atomic pairs (As—As, As—S, and S—S)? (2) If any samples exhibit chemical order, what are the structural units which link to form the glass? (3) Do these units have different forms at different alloy compositions?

Perhaps more important than answering these particular questions is the more global issue addressed: the importance of chemical order in determining material properties. Our studies and results will demonstrate the strength of viewing these amorphous materials in terms of their chemical order. Indeed, we submit that chemical order lies at the heart of our understanding of the As_xS_{1-x} system, and for systems where such considerations are applicable, the notion of chemical order provides a powerful framework for understanding. In other words, the arsenic-sulfur glass-forming region studied spans a range of materials that are best thought of as strongly chemically ordered glasses where material properties are closely coupled to the chemical species comprising the amorphous network.

In the following, we discuss the notion of chemical ordering in the As-S system in terms of x-ray-absorption spectroscopy experiments. In Sec. II we describe our experiment. Section III describes our data analysis, while Sec. IV presents the results and discussion. We conclude in Sec. V.

II. EXPERIMENT

A. Sample preparation

High-purity c-As and c-S (both 99.999%) were obtained from the Alpha Company. Samples of As_xS_{1-x} were placed in fixed proportions into quartz tubes (6-mm outer diameter) in a nitrogen-purged glove box. In order to ensure high cooling rates, sample mass was limited to about 200 mg. Ampoules were heated in a rocking furnace at 650 °C for about 24 h to assure a homogeneous, low-viscosity melt and then ice-water quenched before being returned to room temperature. Samples of As_xS_{1-x} of compositions corresponding to x values of 0.20, 0.30, 0.40, 0.42, 0.43, 0.45, and 0.50 were prepared.

The structural phase of samples was checked by x-ray diffraction using Cu $K\alpha$ radiation. Because there were no detectable Bragg reflections, the glassy samples ($x \leq 0.43$) were confirmed to be amorphous. A few crystalline peaks (which are possibly attributable to c-As_4S_4) were found for the case of the alloys $As_{0.45}S_{0.55}$ and $As_{0.50}S_{0.50}$. Transmission-electron microscopy (TEM) was used to check for phase separation in the As-rich alloys. TEM samples were prepared by grinding the material in an agate mortar and pestle. The powders were then suspended in alcohol and floated onto a Cu grid for the analysis in the TEM using a JEOL 100 electron microscope equipped with a Gatan 607 electron-energy-loss spectrometer and energy-dispersive spectrometer.

For XAS studies, samples were separately ground to fine powders to pass 400 mesh, and then spread uniformly onto Kapton tape. Various thicknesses of samples were routinely measured to determine a range for which the amplitude of the extended x-ray-absorption fine structure (EXAFS) did not change. The thicknesses of samples for the XAS measurements were also determined by statistical considerations which optimized the signal-to-noise ratio. Typically about six to eight layers of tape were used to make samples of sufficient thickness for the x-ray-absorption measurements.

B. XAS measurements

XAS measurements at the K edge of As were made on the National Synchrotron Light source at Brookhaven National Laboratory on the X-11A beam line. During the measurements, the synchrotron was typically operated at an energy of 2.5 GeV and a current between 40 and 80 mA. Energy selection was accomplished by using a double-crystal monochromator with Si(111) crystals. The photon energy was initially calibrated with the first inflection point of the Cu K edge at 8979 eV. Energy resolution was 1.5 eV for the near-edge structure and about 3.0 eV for the EXAFS. For the Si(111) crystals used, the second harmonic is forbidden and the beam contains only the fundamental (111) and the third harmonic (333). In order to filter out unwanted harmonics, the angle between the monochromator crystal faces must be adjusted to detune the incident beam by 20%. The beam incident on the sample was approximately 0.5×15 mm^2, and both incident and transmitted x-ray intensities were measured simultaneously in different ionization chambers. The energy calibration of the monochromator was regularly checked by placing a sample of c-As directly in front of a third ionization chamber where the As K edge was monitored. The first ionization chamber was filled with about 20% argon and 80% nitrogen while the second and third ionization chambers contained only argon. The signals induced by photoionization events in the chambers were amplified by a Keithley current

amplifier and converted to digital form for storage in a PDP 11/34 computer. Transmission spectra on each sample were taken at liquid-nitrogen temperature and room temperature, and each sample was subjected to at least four different scans to estimate the noise.

III. DATA ANALYSIS

Details of EXAFS data reduction have been described elsewhere.[8,9] The x-ray-absorption data as a function of photon energy are processed in the standard way consisting of the preedge subtraction, normalization, removal of EXAFS background, conversion to k space, Fourier transformation, and Fourier filtering to isolate the EXAFS contributions of the shell or shells to be analyzed from that of other shells. The EXAFS spectrum is given by

$$\chi(k)=-\sum_i \frac{N_i F_i D_i(k) e^{-2k^2\sigma_i^2}}{kR_i^2}\sin[2kR_i+\phi_i(k)] \ . \quad (1)$$

In this representation, k is the electron wave vector, $F_i(k)$ is the backscattering amplitude from each of the N_i equivalent neighbors of type i which are located at an average distance R_i from the absorbing atom, σ_i^2 is the Debye-Waller term, and $\phi_i(k)$ is the total phase shift including central-atom and backscatterer contributions. The factor $D_i(k)$ takes account of the effect of inelastic processes. In order to determine the structural parameters, R, N, and σ_i^2, two methods are used: (a) the ratio method and (b) the nonlinear least-squares fitting with the aid of phase-corrected Fourier transform (PCFT).[9] The analysis herein uses an empirical approach for determining the phase and amplitude functions. The empirical approach involves choosing good standards. The criteria for a standard to be good includes having the same absorbing and backscattering atom, the same number of atoms in the first coordination shell, and an approximately equal average distance and a similar chemical state as the unknown. In our studies, the standards used are c-As and c-As_2S_3.

A. The ratio method

If only a single type of scatterer is present in a given shell and the interatomic distances of the sample and standard are similar, by taking the logarithm of the ratio[10] of the isolated shell amplitudes of the sample and standard one obtains

$$\ln\left[\frac{\chi_u(k)}{\chi_s(k)}\right]=\ln\left[\frac{N_u}{N_s}\right]+2k^2(\sigma_s^2-\sigma_u^2) \ . \quad (2)$$

Here u and s denote the unknown and standard samples, respectively. Plotting the logarithm of the ratio of the amplitudes versus k^2 should yield a straight line which has an intercept of $\ln(N_u/N_s)$ and is of slope $2(\sigma_s^2-\sigma_u^2)$. Since N_s and σ_s^2 are presumed to be known, the structural parameters N_u and σ_u^2 are obtained in a straightforward manner. In Fig. 1 we show plots of the logarithm

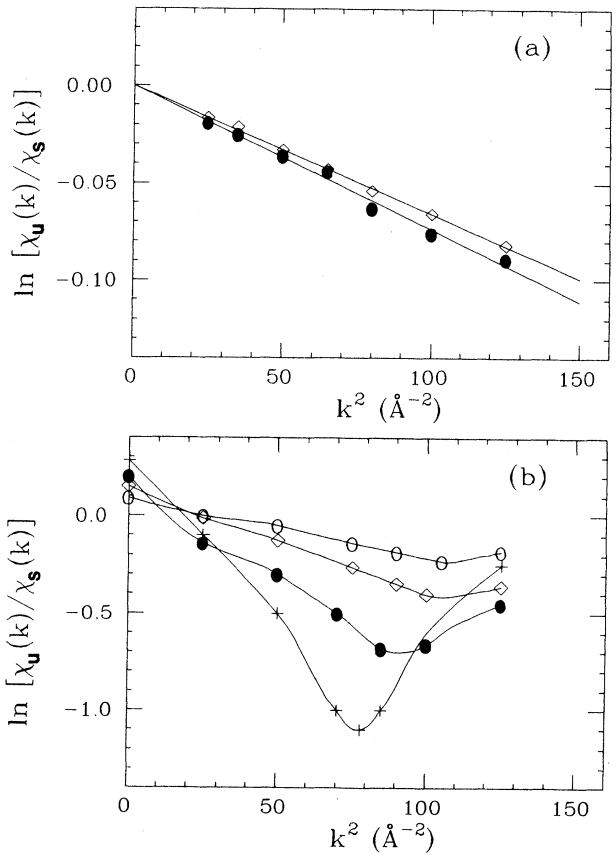

FIG. 1. The logarithm of the ratio of the isolated first shell EXAFS amplitude vs k^2 for (a) S-rich alloys, $As_{0.20}S_{0.80}$ (open diamonds) and $As_{0.30}S_{0.70}$ (solid dots); and (b) As-rich alloys, $As_{0.42}S_{0.58}$ (open circles), $As_{0.43}S_{0.57}$ (open diamonds), $As_{0.45}S_{0.55}$ (solid circles), and $As_{0.50}S_{0.50}$ (crosses). Note the compositional trend of the deviations from linearity in the high-k region of the data for As-rich alloys. This strongly indicates the presence of As scatterers. The first shell (As-S) of c-As_2S_3 is used as a standard.

of the amplitude ratio for the first shell of As_xS_{1-x} alloys using c-As_2S_3 as a standard for the As—S pairs. Note that in Fig. 1(a), good straight lines are obtained for g-$As_{0.20}S_{0.80}$ and for g-$As_{0.30}S_{0.70}$. This is due to the fact that the EXAFS contribution for the first shell for S-rich glasses arises mainly from the As—S pairs. For As-rich samples seen in Fig. 1(b) a change from negative slopes to positive slopes occurs at high k. This is caused by the fact that another type of scatterer (an As atom) begins to dominate in this As-rich region. Thus, we see that the ratio method provides a tool to "fingerprint" the existence of other types of neighbors in binary As_xS_{1-x} systems.

B. Fitting with the PCFT method

In the case of As-rich alloys in which S and As atoms are mixed in the first shell, an alternative approach involves filtering data and fitting to standards (c-As_2S_3 and c-As) using the phase-corrected Fourier-transform

method. In this method, one uses a nonlinear least-squares approach to minimize the difference, D, between the experimental data χ^e and the fitted function χ^f. D is given by

$$D=\sum_i (\chi_i^e-\chi_i^f)^2 W_i \ . \tag{3}$$

Here the sum is taken over the data points i being used for the data analysis and W_i is a weighting function. Two problems which could lead to false conclusions in multishell fits are (1) parameter correlation and (2) local-minima effects. The fitting procedure postulates initial assumptions involving the number of shells and type of scatterers. Each shell usually requires four parameters: R, N, σ^2, and an inner potential E_0. It is well known that R and E_0, as well as N and σ^2, are highly correlated with each other for a given shell. If one introduces more unconstrained parameters into the fits, these parameters would cross-correlate, such that the significance of individual values would be questionable. A second problem is that of obtaining a global minimum in the fitting procedures. The difference in Eq. (3) is minimized via an optimization program. Analytically, a minimum in D may be obtained from a set of variables which may not represent a global minimum. In order to assess the accuracy of the data analysis, the PCFT is used to help test the reliability of the final fitting result. This method benefits from the sensitivity of the phase-shift function. For this study, we are fortunate since the difference in phase shift between As-S and As-As scattering is approximately π radians. This helps us to identify the species of neighboring atom (As and/or S), which in turn allows us to separate the As-S and As-As pair-distribution functions contributing to the first shell. This method is accomplished by transforming the EXAFS spectrum after first multiplying data by $\exp[-\phi_i(k)]$ where the phase-shift function for the particular elements being studied is empirically derived from the appropriate standards.

Analysis of g-$As_{0.43}S_{0.57}$ may serve as an example of the PCFT method. For this sample, the total Fourier transform of the EXAFS is shown in Fig. 2(a) while the As-S PCFT appears in Fig. 2(b) and the As-As PCFT in Fig. 2(c). In the uncorrected total transform at the top [2(a)], a shoulder is seen on the first peak. Separation into As-S and As-As corrected components [2(b) and 2(c), respectively] makes the resolution of two separate contributions evident. The main feature at lower r is due to the sulfur neighbors that have heteropolar bonds to arsenic atoms, while the higher-r feature is due to arsenic neighbors with homopolar bonds.

The fit for the PCFT analysis of Fig. 2(a) used the EXAFS over a k range of 4–14 Å^{-1}, beginning with the experimental data shown as the solid line in Fig. 3. In this figure, the EXAFS is shown with a k^3 weighting. Our ability to accurately identify the separate contributions to the first shell is demonstrated in two distinct ways. First, an examination of the behavior of the imaginary part of the transform (the dashed lines in Fig. 2) reveals a symmetric behavior of this imaginary component for both the As-S corrected and the As-As corrected transforms. Furthermore, the imaginary part of the transform is maximized at the same value as the total transform. These facts imply that the PCFT has cleanly separated the shell into distinct components. In the total transform of Fig. 2(a), the imaginary contribution does not show the symmetric behavior and is indicative of a mixture of components. Further substantiation of the accuracy of the resolution of the separate components lies in an examination of the best fit of the Fourier transform of the sum of the separately resolved components in k space. This fit is shown as crosses in Fig. 3. The crosses match very well the experimental data given as the solid line. Slight deviations at high k are amplified by the k^3 weighting.

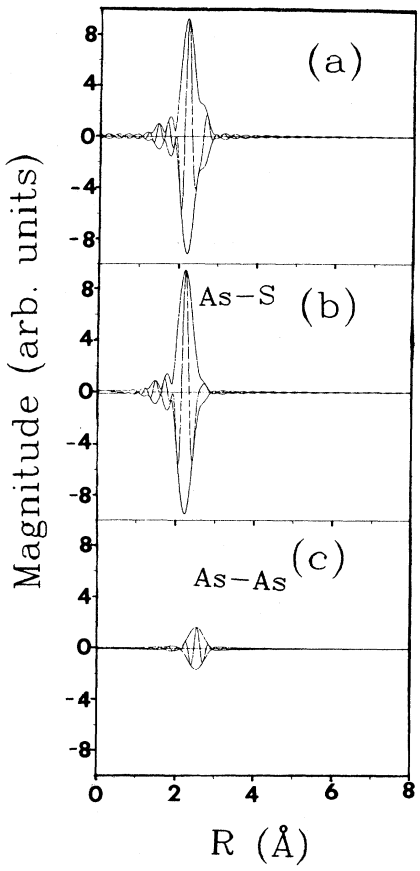

FIG. 2. The imaginary part and the magnitude of the Fourier transforms $k^3\chi(k)$ of the isolated first shell of g-$As_{0.43}S_{0.57}$. All transforms were done over a k-space range of 2.6–14.4 Å^{-1} for (a) the As-S PCFT spectra, (b) the residual of the As-S PCFT spectra, and (c) the residual of the As-As PCFT spectra. Detailed analysis are described in the text.

In fitting the data as was done in Figs. 2 and 3, we determined the coordination numbers (N), bonding distances (R), and Debye-Waller factors ($\Delta\sigma^2$) for each subshell separately. For the As-As contribution, we find

$$N_{\text{As-As}}=0.3 \ ,$$

$$R_{\text{As-As}}=2.56 \ \text{Å} \ ,$$

$$\Delta\sigma^2=-0.0002 \ \text{Å}^2 \ .$$

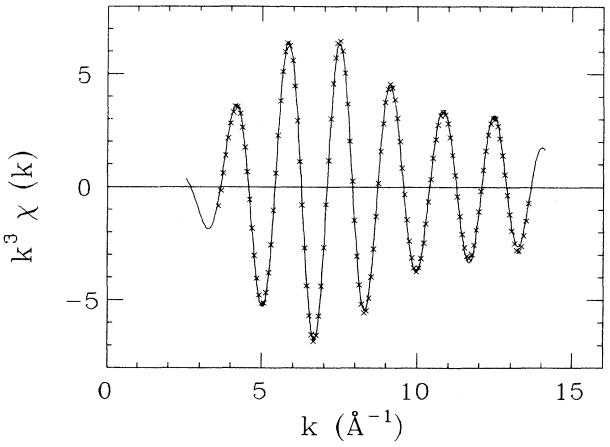

FIG. 3. Comparisons of $k^3\chi(k)$ for experimental data (solid line) and a nonlinear least-squares fit (crosses) of g-$As_{0.43}S_{0.57}$.

While for the As-S contribution

$N_{\text{As-S}}=2.7$,

$R_{\text{As-S}}=2.27$ Å ,

$\Delta\sigma^2=0.0003$ Å^2 .

IV. RESULTS AND DISCUSSION

A. The S-rich region ($x<0.40$)

Both the EXAFS data multiplied by k^3 and the As-S PCFT's for three glasses studied (g-$As_{0.20}S_{0.80}$, g-$As_{0.30}S_{0.70}$, and g-$As_{0.40}S_{0.60}$) are shown in Figs. 4 and 5. Using the ratio and the nonlinear least-squares fitting method for the data filtered from the Fourier transform in the region of 1.6–3.0 Å, it is found that the As environment in S-rich glasses is similar to that of c-As_2S_3. The results are listed in Table I. In Fig. 5, the first main peaks are due to the first As-S shell with As—As bonds undetectable in S-rich glasses. This suggests that the local AsS_3 structure is preserved. Our results contradict the argument that a certain number of AsS structural units having As—As bonds are present in S-rich glasses as suggested by Kosek *et al.*[11] It is readily apparent from the transform spectra that the magnitude of the first shell peak is somewhat smaller for g-$As_{0.30}S_{0.70}$ than for g-$As_{0.20}S_{0.80}$. It seems likely that the thermal disorder in the S-rich glasses is similar to that in c-As_2S_3, since the As-S stretching forces[12] are so similar. Thus, the difference in $\Delta\sigma^2$ between g-$As_{0.20}S_{0.80}$ and g-$As_{0.30}S_{0.70}$ is probably due to differences in structural disorder in the connectivity of the AsS_3 units, presumably due to —S—S—S— linkages.

Because of the large structural and thermal disorder, it is not possible to quantitatively obtain a coordination number for the second shell of g-$As_{0.20}S_{0.80}$ and g-$As_{0.30}S_{0.70}$. It is possible to determine, however, the type

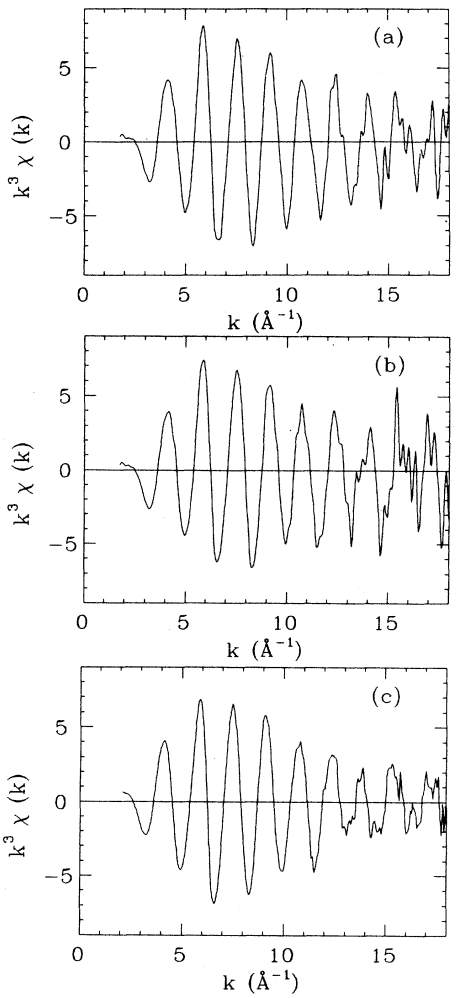

FIG. 4. The $k^3\chi(k)$ spectra for (a) g-$As_{0.20}S_{0.80}$, (b) g-$As_{0.30}S_{0.70}$, and (c) g-$As_{0.40}S_{0.60}$.

of scatterer and its distance. Using the PCFT method, the As-S phase-corrected transform gives a positive peak in the imaginary part as shown in Fig. 5(a), while the As-As corrected transform results in a negative peak in the imaginary part for the second shell. Therefore, this well-defined peak for the second-neighbor As—S distance at 3.80 Å arises from As—S—S linkages. This fact suggests the existence of S—S homopolar bonds. Using the fitting method, detailed analysis indicates that satellites of this peak in the region 3.2–3.6 Å are due to small contributions from As scattering at 3.50 Å indicating the presence of As—S—As linkages. As shown in Fig. 5(b) for the g-$As_{0.30}S_{0.70}$ sample, however, the strong interference between the signal arising from both the As—S—As and the As—S—S linkages makes identification of the signature of homopolar bonding at 3.8 Å less certain. It does appear, however, that there are very few As—S—S linkages in this material. In Fig. 5(c), the second peak of the radial structure function for the g-$As_{0.40}S_{0.60}$ sample exhibits[8] only a well-defined peak which arises from As

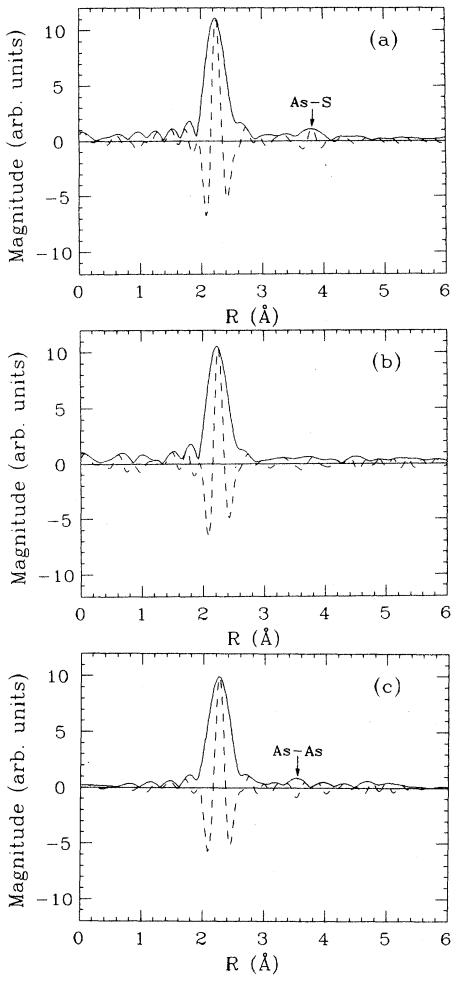

FIG. 5. The As-S PCFT's of the imaginary part (dashed line) and magnitude (solid line) of transforms corresponding to Fig. 4. The k^3 transforms were taken over a range of 2.6–14.4 Å^{-1}. The feature at $R = 3.8$ Å which rises above the noise only for g-$As_{0.20}S_{0.80}$ results from the As—S—S linkages, whereas the feature at $R = 3.5$ Å for g-$As_{0.40}S_{0.60}$ is due to the contribution from the second-As-neighbor shell. In g-$As_{0.30}S_{0.70}$, both the As—S—As and As—S—S features are uncertain due to strong interference.

scattering. We find no such As—S—S linkage in g-$As_{0.40}S_{0.60}$. Meyers and Felty[4] suggest that the structures of S-rich alloys consist of a mixture of aggregates of AsS_3 linkages and S monomer rings when a sufficient amount of S has been added. Lucovsky *et al.*[3] have further suggested that the S_8 ring molecules begin to form at higher concentration, i.e., $x = 0.80$, in the S-rich glasses. We have been unable, however, to identify the S_8 ring molecules from the current data. A study of the K edge of S will be made in the near future.

From both of the features of the first and second shell, we are therefore lead to the conclusion that for S-rich samples only As—S and S—S bonds are found. This is strong evidence that the chemically ordered network model is appropriate to describe the bond distribution for S-rich compositions. For $x = 0.70$, sulfur atoms are incorporated in the chains linking the pyramidal molecules. The S atoms simply become additional links in chain segments. At higher concentrations ($x = 0.80$) some As-S-As linkages are replaced by As—S—S linkages.

B. The As-rich region ($x > 0.40$)

The EXAFS data weighted by k^3 for As-rich samples ($x = 0.42$, 0.43, 0.45, and 0.50) and for c-As_4S_4 are shown in Fig. 6. The corresponding As-S PCFT's are shown in Fig. 7. The predominant contributions to the first shell of the As-S PCFT's for g-$As_{0.42}S_{0.58}$ and for g-$As_{0.43}S_{0.57}$ are due to As—S bonds at 2.27 Å, while the additional features causing the shoulder in the first shell are due to As—As bonds at 2.56 Å. The As-S PCFT of c-As_4S_4 shows two major peaks, one at 2.24 Å due to contributions from two As—S bonds and one at 2.57 Å due to the contribution from one As—As bond. It can be seen in Fig. 7 that a well-defined shoulder on the high-r side of the first peak in the As-rich samples grows rapidly with increasing As content, clearly becoming a distinct peak for $As_{0.45}S_{0.55}$ and $As_{0.50}S_{0.50}$ alloys. Similar changes in the second shell are also seen. The contributions of the As—S and As—As bonds to the first shell for As-rich alloys were determined by the PCFT method and are summarized in Table II. A major difference among the As-rich samples is the increasing contribution of As—As bonds and the decreasing contribution of As—S bonds in

TABLE I. Structural parameters for g-$As_{0.20}S_{0.80}$, g-$As_{0.30}S_{0.70}$, and g-$As_{0.40}S_{0.60}$ alloys.

Sample	Shell	Bond	N	R (Å)	$\Delta\sigma^2$ (10^{-4} Å^{-2})[a]
g-$As_{0.20}S_{0.80}$	1	As—S	3.0±1	2.27±0.01	1±2
	2	As—As	b	3.5±0.1	b
	2	As—S	b	3.8±0.1	b
g-$As_{0.30}S_{0.70}$	1	As—S	3.0±0.1	2.27±0.01	7±2
	2	As—As	b	3.5±0.1	b
	2	As—S	b	3.8±0.1	b
g-$As_{0.40}S_{0.60}$	1	As—S	3.0±0.1	2.28±0.01	6±2
	2	As—As	b	3.5±0.1	b

[a]Relative structural disorder with respect to c-As_2S_3.
[b]Indeterminate.

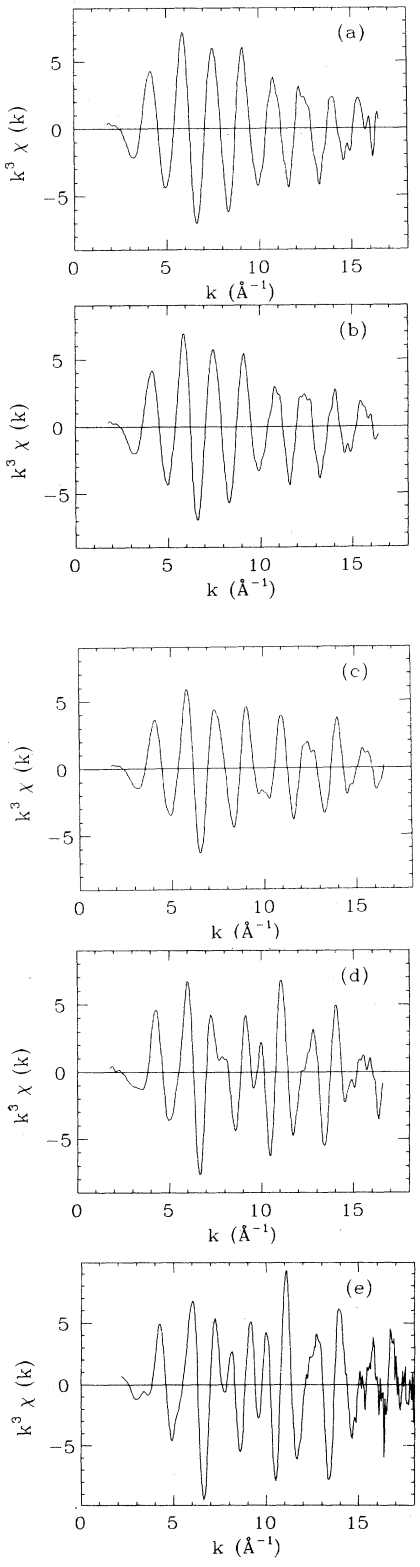

FIG. 6. The $k^3\chi(k)$ spectra for (a) g-$As_{0.42}S_{0.58}$, (b) g-$As_{0.43}S_{0.57}$, (c) $As_{0.45}S_{0.55}$, (d) $As_{0.50}S_{0.50}$, and (e) c-As_4S_4. From qualitative comparisons it can be seen that g-$As_{0.42}S_{0.58}$ and g-$As_{0.43}S_{0.57}$ have similar spectra.

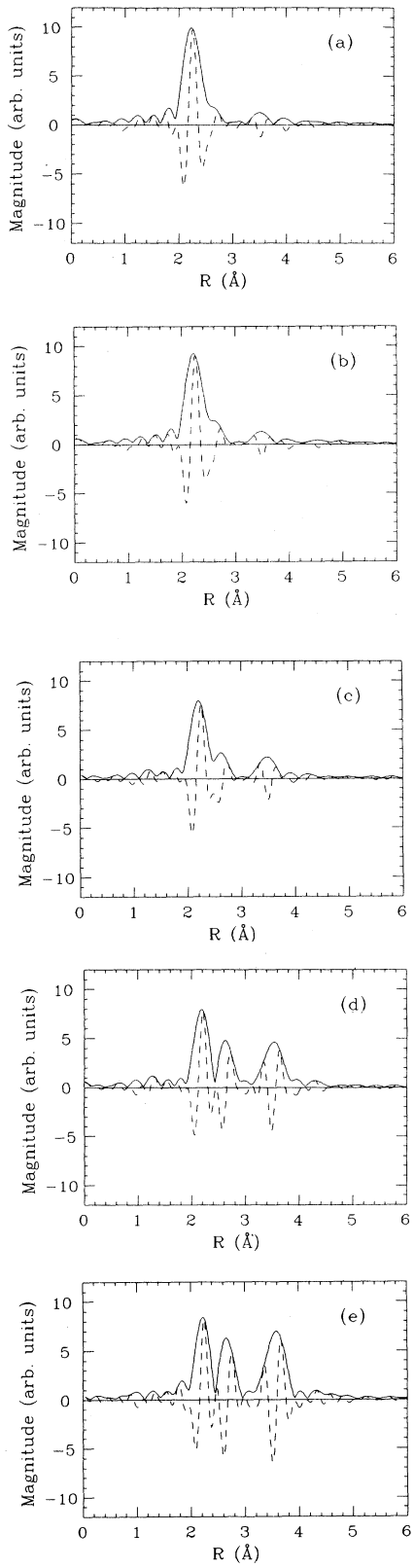

FIG. 7. The As-S PCFT's corresponding to Fig. 6. The k^3 transforms were taken over a range of 2.6–14.4 Å^{-1}.

TABLE II. Structural parameters for g-$As_{0.42}S_{0.58}$, g-$As_{0.43}S_{0.57}$, $As_{0.45}S_{0.55}$, and $As_{0.50}S_{0.50}$ alloys.

Sample	Shell	Bond	N	R (Å)	$\Delta\sigma^2$ (10^{-4} Å^{-2})
g-$As_{0.42}S_{0.58}$	1	As—S	2.8±0.1	2.27±0.02	4±5
	1	As—As	0.2±0.1	2.56±0.02	−3±5
	2	As—As	3.0±0.5	3.50±0.02	35±10
g-$As_{0.43}S_{0.57}$	1	As—S	2.7±0.1	2.27±0.02	3±5
	1	As—As	0.3±0.1	2.56±0.02	2±5
	2	As—As	3.1±0.5	3.50±0.02	32±10
$As_{0.45}S_{0.55}$	1	As—S	2.5±0.1	2.26±0.02	−2±5
	1	As—As	0.5±0.1	2.57±0.02	2±5
	2	As—As	3.4±0.5	3.52±0.02	59±10
	2	As—S	0.9±0.5	3.58±0.02	48±10
$As_{0.50}S_{0.50}$	1	As—S	2.0±0.1	2.24±0.02	−2±5
	1	As—As	1.0±0.1	2.57±0.02	6±5
	2	As—As	3.6±0.5	3.54±0.02	74±10
	2	As—S	1.6±0.5	3.58±0.02	34±10

the first shell with increasing As content. Structural changes associated with composition indicate that a breakdown of the AsS_3 linked network is observed and the formation of As—As bonds is evident.

An important question in the study of the role of As atoms in As-rich samples is whether the formation of As—As bonds is due to the presence of wrong bonds in the network (i.e., As—S—As linkages being replaced by S—As—As—S linkages) or is due to the existence of As_4S_3 or As_4S_4 molecules, both of which have As—As bonds. The results at hand address this issue directly. The relatively long As—As bond distances (2.56±0.02 Å) observed by us in g-$As_{0.42}S_{0.58}$ and g-$As_{0.43}S_{0.57}$ are similar to that found[11] in c-As_4S_4 (2.57 Å). In addition, the As—As bond distances (2.57±0.02 Å) observed in $As_{0.45}S_{0.55}$ and $As_{0.50}S_{0.50}$ alloys are the same as those found in c-As_4S_4. The somewhat shorter As—As bond distance (2.45 Å) indicative of As_4S_3 molecules[13] is not observed in our transforms. Since the identification of any species is made according to relative abundance, however, we cannot rule out the existence of As_4S_3 molecules[14,15] as minor constituents (below a few atomic percent). Also ruled out as principal constituents of our alloys are a-As and c-As where the normal covalent-bond distances[16] are 2.49 and 2.51 Å, respectively.

Ito and co-workers[17] have pointed out that although the structures of c-As_4S_4 and c-As_2S_3 have superficially little similarity, they are in fact built from the same structural units but on a different principle. The two halves of cradle-type molecules of As_4S_4 are arranged in spiral chain configurations in As_2S_3, with the atoms arranged in alternating As—S—As—S—As order. A rotation of one-half of such a cradle about a diagonal axis passing through the center of the molecule would bring the atoms in approximate coincidence with an As_4S_4 molecule. Furthermore, it has been suggested[18,19] that vapor-deposited amorphous As_2S_3 films contain As_4S_4 molecules bonded by van der Waals forces with the network formed principally of AsS_3 units. The formation of As_4S_4 molecular species in a network of AsS_3 elements is therefore reasonable. The above evidence suggests that the excess of As in glassy As-rich alloys, which necessarily results in an increase in As—As bond population at the expense of As—S bonds, leads principally to the formation of As_4S_4 molecules.

It has been shown[14,20] that the Raman spectra of As-rich alloys change very smoothly with As content. This has raised the question as to whether microcrystals of As_4S_4 or discrete randomly oriented As_4S_4 molecules (or perhaps mixtures of molecules in a microcrystalline matrix) are formed in the As-rich alloys. Structural information in the second shell provides important clues in addressing this question. As a function of increasing As content, there are measurable structural changes. Using the fitting method in the region of 3–4 Å, we find that the coordination of nonbonded As—As pairs, as well as nonbonded As—S pairs, increase with increasing As content as indicated in Table II. In Fig. 7(e), the As-S transform shows that the second broad peak in c-As_4S_4 represents contributions from intramolecular and intermolecular neighbors. The mean values of intramolecular second-shell distances are 3.45 and 3.67 Å for the two As—As pairs and the two As—S pairs, respectively. The corresponding intermolecular distances are 3.57 and 3.58 Å for As-As ($N=1.8$) and As-S ($N=2.3$), respectively. As seen from Table II, a short-range structural similarity between the $As_{0.50}S_{0.50}$ specimen and c-As_4S_4 (realgar) is manifest; however, the coordination numbers for both As-As and As-S are reduced for the $As_{0.50}S_{0.50}$ sample. These data are consistent with a structure in which As_4S_4 molecular fragments (call this g-As_4S_4) coexist with microcrystalline As_4S_4. The g-As_4S_4 units are arranged in a random way—quite unlike the molecules in c-As_4S_4. Some of the intermolecular atomic correlations are below detectable limits because of the large static and dynamic disorder of the g-As_4S_4 units in the $As_{0.50}S_{0.50}$ specimen.

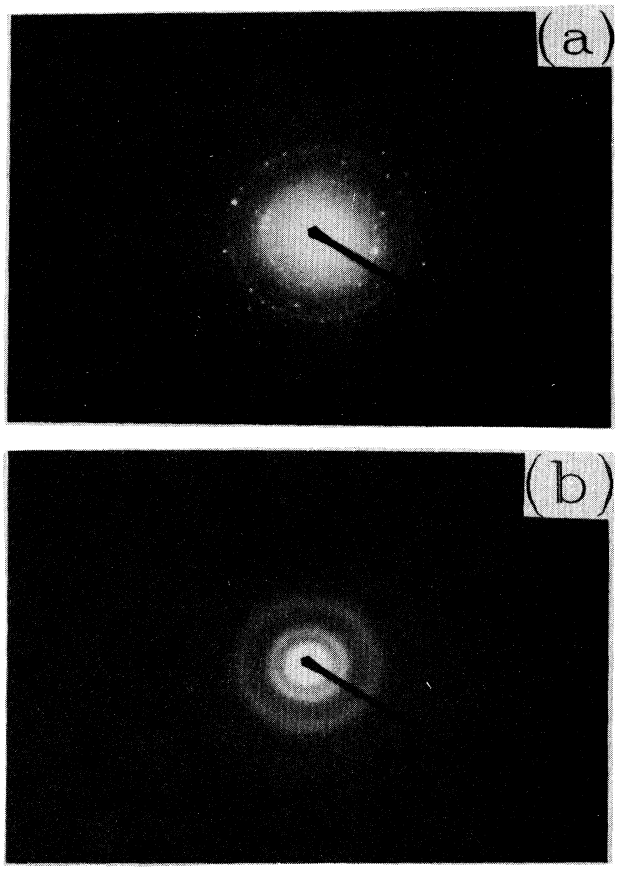

FIG. 8. Diffraction patterns of two structural phases of the $As_{0.50}S_{0.50}$ alloy for (a) c-As_4S_4 and (b) g-As_4S_4.

The $As_{0.50}S_{0.50}$ sample contains very few As_2S_3 units, if any. Indeed, only two structural phases seen in the transmission micrograph are c-As_4S_4 and g-As_4S_4. Diffraction patterns of these two structural phases, c-As_4S_4 and g-As_4S_4, are shown in Fig. 8. Three diffuse halos can be seen in Fig. 8(b). The image of the $As_{0.50}S_{0.50}$ sample shows that the crystalline particle size of c-As_4S_4 is on the order of 100 Å, where the g-As_4S_4 region is less than 50 Å.

Unanswered from this study is the nature of the coupling between the network forming units of AsS_3 and the As_4S_4 molecules in slightly As-rich samples. Further insights such as these must await further experimental results. In a homogeneous glass structure for g-$As_{0.42}S_{0.58}$ and g-$As_{0.43}S_{0.57}$, the g-As_4S_4 must of course be randomly dispersed throughout the matrix. What is clear from our study is the fact that when the composition is more than 43 at. % As, microcrystals of c-As_4S_4 are formed. These results are in agreement with several Raman studies.[3,14,20,21]

V. CONCLUSIONS

In conclusion, the following general statements can be made in reference to the compositional dependence of the structure of glassy As_xS_{1-x}: in the S-rich region, the local structure consists of AsS_3 configurations linked together through a number of S—S bonds. For slightly As-rich alloys ($0.40 < x < 0.43$), As_4S_4 molecular fragments (g-As_4S_4) are randomly dispersed throughout a network comprised of AsS_3 pyramids which are linked by common S atoms. From our data we are unable to determine the nature of the coupling between the network forming units of AsS_3 and the As_4S_4 molecules in slightly As-rich samples. For more heavily As-rich samples ($x = 0.45$ or 0.50), g-As_4S_4 coexist with microcrystalline As_4S_4. The g-As_4S_4 units are arranged in a random way—quite unlike the molecules in c-As_4S_4. Some of the intermolecular atomic correlations in the $As_{0.50}S_{0.50}$ specimen are below detectable limits of our experiments, but we can conclude that the $As_{0.50}S_{0.50}$ sample contains very few As_2S_3 units, if any.

ACKNOWLEDGMENTS

The authors would like to thank Professor E. A. Stern and Professor G. Lucovsky for helpful discussions. Special thanks go to Bob Sabatini for performing TEM measurements. This work is supported in part by the National Science Foundation under Grant No. DMR-8407265 and the Department of Energy under Contract No. DE-AS05-80ER10742, which also supported the development of the X-11A beam line at the National Synchrotron Light Source. The National Synchrotron Light Source is supported by the U.S. Department of Energy, Division of Materials Sciences, and Division of Chemical Sciences under Contract No. DE-AC02-76CH00016.

*Mailing address: Bldg. 480, Brookhaven National Laboratory, Upton, New York 11973.

[1]W. H. Zachariasen, J. Am. Chem. Soc. **54**, 3841 (1932).
[2]R. M. White, J. Non-Cryst. Solids **16**, 387 (1974).
[3]G. Lucovsky, F. L. Galeener, R. H. Geils, and R. C. Keezer, in *The Structure of Non-Crystalline Materials* (Taylor and Francis, London, 1977), p. 127.
[4]B. M. Myers and E. J. Felty, Mater. Res. Bull. **2**, 535 (1967).
[5]J. P. DeNeufville and H. K. Rockstad, in *Amorphous and Liquid Semiconductors,* edited by J. Stuke and W. Brenig (Taylor and Francis, London, 1974).
[6]K. Shimakawa, J. Non-Cryst. Solids **43**, 229 (1981).
[7]M. Yamaguchi, Philos. Mag. B **51**, 651 (1985).
[8]C. Y. Yang, D. E. Sayers, and M. A. Paesler, Phys. Rev. B **36**, 8122 (1987).
[9]C. Y. Yang, M. A. Paesler, and D. E. Sayers, Phys. Rev. B **36**, 9160 (1987).
[10]Grant Bunker, Nucl. Instrum. Methods **207**, 437 (1983); E. A. Stern, D. E. Sayers, and F. W. Lytle, Phys. Rev. B **11**, 4836 (1975).
[11]F. Kosek, J. Chlebny, Z. Cimpl, and J. Mavek, Philos. Mag. B **47**, 627 (1983).

[12]C. Y. Yang, M. A. Paesler, and D. E. Sayers, Phys. Rev. B **36**, 980 (1987).
[13]H. J. Whitfield, J. Chem. Soc., Dalton Trans. 1740 (1973).
[14]P. J. S. Ewen, M. J. Sik, and E. A. Owen, Solid State Commun. **33**, 1067 (1980).
[15]A. T. Ward, Adv. Chem. **110**, 163 (1972).
[16]G. N. Greaves, S. R. Elliott, and E. A. Davis, Adv. Phys. **28**, 49 (1978).
[17]T. Ito, N. Morimoto, and R. Sadanga, Acta Crystallogr. **5**, 775 (1952).
[18]R. J. Nemanich, G. A. N. Connell, T. M. Hayes, and R. A. Street, Phys. Rev. B **18**, 6900 (1978).
[19]C. Y. Yang, J. M. Lee, M. A. Paesler, and D. E. Sayers, J. Phys. (Paris) Colloq. **47**, C8-387 (1986).
[20]A. Bertouzza, C. Fagnano, P. Monti, and G. Semerano, J. Non-Cryst. Solids **29**, 49 (1978).
[21]A. T. Ward, J. Phys. Chem. **72**, 4133 (1968).

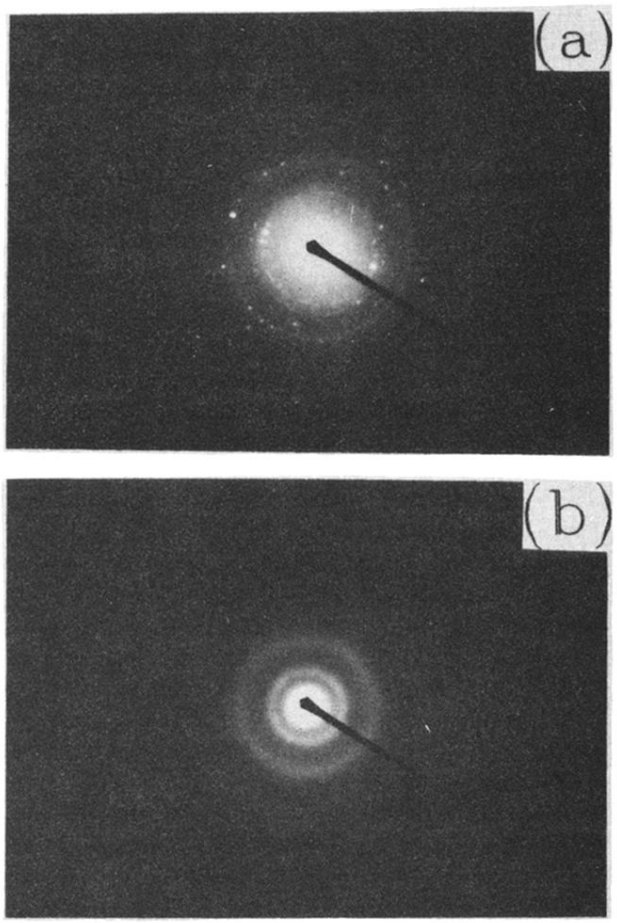

FIG. 8. Diffraction patterns of two structural phases of the $As_{0.50}S_{0.50}$ alloy for (a) c-As_4S_4 and (b) g-As_4S_4.